JACS
JOURNAL OF THE AMERICAN CHEMICAL SOCIETY

Communication

pubs.acs.org/JACS

Direct Electrodeposition of Crystalline Silicon at Low Temperatures

Junsi Gu,[†] Eli Fahrenkrug,[†] and Stephen Maldonado*[,†,‡]

[†]Department of Chemistry and [‡]Program in Applied Physics, University of Michigan, 930 North University Avenue, Ann Arbor, Michigan 48109-1055, United States

Supporting Information

ABSTRACT: An electrochemical liquid–liquid–solid (ec-LLS) process that yields crystalline silicon at low temperature (80 °C) without any physical or chemical templating agent has been demonstrated. Electroreduction of dissolved $SiCl_4$ in propylene carbonate using a liquid gallium [Ga(*l*)] pool as the working electrode consistently yielded crystalline Si. X-ray diffraction and electron diffraction data separately indicated that the as-deposited materials were crystalline with the expected patterns for a diamond cubic crystal structure. Scanning and transmission electron microscopies further revealed the as-deposited materials (i.e., with no annealing) to be faceted nanocrystals with diameters in excess of 500 nm. Energy-dispersive X-ray spectra further showed no evidence of any other species within the electrodeposited crystalline Si. Raman spectra separately showed that the electrodeposited films on the Ga(*l*) electrodes were not composed of amorphous carbon from solvent decomposition. The cumulative data support two primary contentions. First, a liquid-metal electrode can serve simultaneously as *both* a source of electrons for the heterogeneous reduction of dissolved Si precursor in the electrolyte (i.e., a conventional electrode) *and* a separate phase (i.e., a solvent) that promotes Si crystal growth. Second, ec-LLS is a process that can be exploited for direct production of crystalline Si at much lower temperatures than ever reported previously. The further prospect of ec-LLS as an electrochemical and non-energy-intensive route for preparing crystalline Si is discussed.

Presently, the major industrial method for the production of crystalline silicon, the key semiconductor in many optoelectronic technologies, involves a series of energy-intensive, highly polluting carbothermal reduction reactions that produce undesirable byproducts, including CO_2.[1,2] Electrodeposition has long been identified as a potential alternative route for the preparation of Si since electrodepositions can be inherently simple, clean, and comparatively non-energy-intensive.[3,4] However, resource-intensive carbothermal reactions are generally still preferred over electrodeposition for Si production for two principal reasons. First, as-prepared Si from low-temperature electrodepositions is often impure with components from the electrolyte at $>10^{-1}$ atom %[5,6] and is always amorphous,[5−14] requiring additional thermal annealing and purification. Second, excessively high (>700 °C) temperatures are required for an electrodeposition process to yield crystalline Si.[15−18] The incompatibility of low temperatures and a pure, crystalline product have thus severely limited the appeal of Si electrodeposition. Accordingly, a new Si electrodeposition method that overcomes this longstanding challenge would be highly desirable and could have substantial technological impact.

We recently reported on the concept of using liquid-metal electrodes that act as *both* an electron source for reducing dissolved species in solution *and* a solvent for recrystallization.[19−21] We have dubbed this strategy an electrochemical liquid–liquid–solid (ec-LLS) process for the direct preparation of crystalline semiconductor materials. This tactic has proven versatile, affording the direct electrodeposition (i.e., reduction of dissolved precursor to give fully reduced crystalline material without need for subsequent annealing) of copious amounts of crystalline Ge and GaAs from an aqueous solution at or near ambient conditions. A key advancement for ec-LLS as a synthetic strategy would be to determine whether a liquid-metal electrode could facilitate the direct preparation of crystalline Si. Accordingly, here we report data demonstrating the use of a liquid-metal electrode as a platform for direct electrodeposition of crystalline Si from a dissolved precursor under relatively benign conditions.

Figure 1a illustrates one possible means for the direct electrodeposition of crystalline Si. As has been demonstrated for Ge[19,20] and GaAs,[21] the initial stage would involve electroreduction of an oxidized precursor ($SiCl_4$) to the fully reduced state (Si) at the electrode–electrolyte interface. Electroreduction of $SiCl_4$ at solid electrodes has been investigated previously[5,6,8,11] and found to produce purely amorphous Si. In the ec-LLS scheme, the initially reduced Si could be partitioned *into* the liquid gallium [Ga(*l*)] phase. The solubility of Si in Ga between room temperature and 100 °C, as determined by extrapolations of published metallurgical data for the Ga–Si system,[22,23] ranges from 10^{-8} to 10^{-6} atom %. Although low, the solubility of Si in Ga at 100 °C is comparable to the solubility in another ec-LLS system (Ge in Hg at room temperature)[24] demonstrated previously.[19] The dissolved Si in Ga(*l*) could then reach saturation and supersaturation conditions if $SiCl_4$ is continually reduced at the electrode–electrolyte interface. When a critical supersaturation condition is reached, phase separation of Si(*s*) from Ga(*l*) followed by crystal growth would occur.

To determine whether any observable for the electroreduction of $SiCl_4$ at Ga(*l*) electrodes would support Figure 1a, a two-compartment electrochemical cell was used to electrodeposit Si onto a Ga(*l*) electrode at several temperatures up to

Received: November 5, 2012
Published: January 24, 2013

   dx.doi.org/10.1021/ja310897r | *J. Am. Chem. Soc.* 2013, 135, 1684−1687

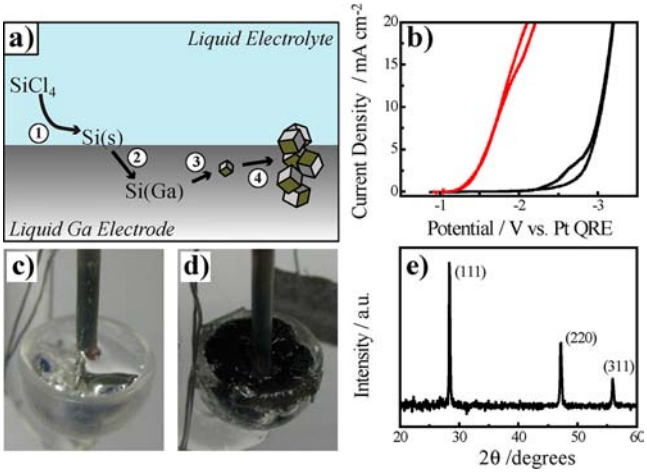

Figure 1. (a) Schematic depiction (not drawn to scale) of an electrochemical liquid–liquid–solid (ec-LLS) process yielding crystalline Si with a liquid Ga [Ga(l)] electrode. (b) Voltammetric response after correction for solution resistance for a Ga(l) electrode in propylene carbonate containing 0.2 M TBACl without (black) or with (red) 0.5 M $SiCl_4$. (c) Optical photograph of a clean Ga(l) working electrode. (d) Optical photograph of the same electrode after galvanostatic electrodeposition of Si in propylene carbonate containing 0.2 M TBACl and 0.5 M $SiCl_4$ at 20 mA cm^{-2} for 2 h at 100 °C. The image was obtained after physical removal from the cell. (e) Representative X-ray diffractogram collected from the black film in (d).

200 °C. The cell was pressurized to 2.76×10^6 Pa (400 psi) to offset the volatility of $SiCl_4$ at elevated temperatures.[25] Figure 1b shows representative voltammograms for a Ga(l) working electrode scanned to negative potentials in propylene carbonate containing 0.2 M tetrabutylammonium chloride (TBACl) with or without 0.5 M $SiCl_4$ at 100 °C. The data have been corrected for the iR drop from solution resistance, as measured by impedance analysis [Figure S1 in the Supporting Information (SI)], and are the responses observed after the first scan. The presented voltammetry data differ from results reported for the electroreduction of $SiCl_4$ at a solid Ni electrode[5] in that no diffusion-controlled peak was observed under these conditions. Additional voltammetric analysis indicated that a diffusion-controlled peak at these current densities could be observed only at lower $SiCl_4$ concentrations and lower temperatures (Figure S2). Furthermore, the voltammetric response for the first scan always differed from the responses observed for subsequent scans with the appearance of a prewave at a potential ~0.5 V more positive than the onset of $SiCl_4$ reduction.

Figure 1c,d highlights the optical appearance of a Ga(l) pool electrode before and after a galvanostatic experiment at +20 mA cm^{-2} at 100 °C for 2 h. The mass of the dull black film on the Ga(l) electrode following the galvanostatic deposition was sensitive to the length of the experiment, with a smaller apparent mass collected after shorter experiments. The as-prepared film was physically removed from the surface of the Ga(l) pool electrode, dried, and collected as a powder. After washing/etching of the collected mass to remove solvent, physisorbed electrolyte salt, and native oxide (see the SI), the black powder was stored dry under ambient conditions. Notably, the hue and texture of the collected electrodeposit did not change over time in air (Figure S3). Analogous electrodepositions performed at 25 °C yielded similar dark films whose color changed to grayish yellow over the course of a few hours, as commonly observed for porous, amorphous Si in air.[5,9,10,26] In contrast, electrodepositions performed at 100 °C but at low (ambient) pressure yielded crystalline character analogous to that obtained at high pressure (Figure S4), indicating that temperature rather than pressure is more influential on the observation of crystallinity. Further experiments performed under identical conditions but without potential or current control did not yield any deposit on the Ga(l) electrode surface (Figure S4). Finally, experiments in which films were electrodeposited at room temperature and then heated to 100 °C for 2 h inside the cell also produced pale, white material. The absence of any signatures indicative of crystalline Si in these last control experiments argue for a concerted ec-LLS process in the main experiments that is not equivalent to separate electrodeposition and annealing.

Figure 1e presents a representative powder X-ray diffractogram after correction for the scattering contribution from the underlying support. The corresponding raw X-ray diffraction data are presented in Figure S5. As shown in Figure 1e, the as-deposited mass yielded sharp diffraction patterns in accord with the diamond cubic crystal structure expected for crystalline Si. Using either Rietveld refinement or Scherrer line width analysis, the crystalline domain size inferred from the X-ray diffraction data was large (>100 nm). Repeated electrodeposition experiments performed at temperatures as low as 80 °C showed similar X-ray diffraction patterns (Figure S6). Electrodepositions performed at 25 °C yielded dark films that showed no detectable signatures for crystalline Si in the collected X-ray diffraction patterns. An exhaustive analysis of the crystallinity across a large temperature range is currently in progress. Raman spectra showed both the phonon mode for crystalline Si and a lower-frequency signature suggestive of nonzero amorphous content (Figure S8). Raman measurements were also performed to determine whether the material obtained through electrodeposition also contained a substantial amount of amorphous carbon from the decomposition of solvent at the interface with the Ga(l) electrode. A representative spectrum obtained for the as-prepared (i.e., no etching or washing steps) electrodeposited Si mass (Figure S9) shows no detectable Raman signatures for either amorphous or diamond-like carbonaceous species.[27]

Figure 2a,b presents representative scanning electron microscopy (SEM) images that detail the morphology of the as-electrodeposited Si powder. Uniformly sized grains were consistently observed with total widths of ~500 nm. A fraction of the observed particles appeared fused together along an edge. However, the majority of particles looked unfused but aggregated in large clusters. Nearly every observed grain showed sharp facets, consistent with the premise that each grain constituted a single crystal. Electron backscatter diffraction experiments were attempted in order to determine whether each grain in an aggregate was in fact a uniform single crystal, but the grain sizes were too small for conclusive evidence to be obtained. Instead, transmission electron microscopy (TEM) was performed on individual Si grains. Figure 2c shows a representative high-resolution TEM image. Lattice fringes commensurate with the d_{111} spacing for crystalline Si were observed. A representative selected-area electron diffraction (SAED) pattern obtained along the [011] zone axis is shown in the inset of Figure 2c. The observed diffraction pattern is consistent with a diamond cubic lattice and d_{111} = 3.1 Å, as expected for a single crystal of Si. Every particle observed by

dx.doi.org/10.1021/ja310897r | J. Am. Chem. Soc. 2013, 135, 1684–1687

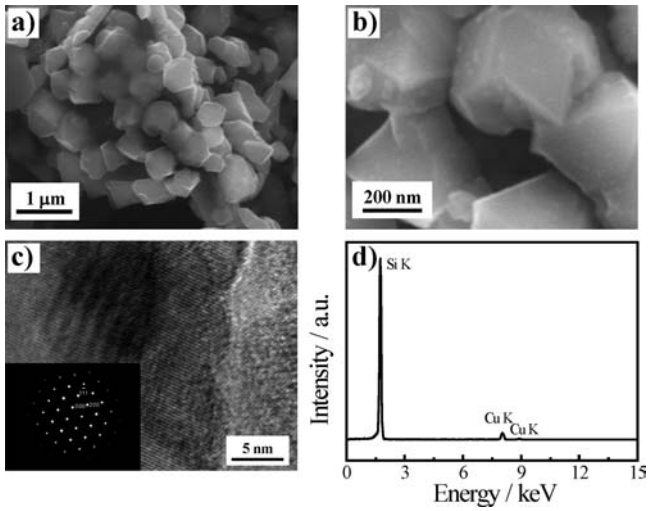

Figure 2. (a, b) SEM images of electrodeposited Si at (a) 20 000× and (b) 80 000× times magnification. (c) High-resolution TEM image of electrodeposited Si at 800 000× magnification. Inset: SAED pattern obtained with the electron beam parallel to the [011] zone axis. (d) EDX spectrum of a crystalline Si grain taken in the transmission electron microscope at 300 kV. Crystalline Si was electrodeposited in a propylene carbonate solution containing 0.2 M TBACl and 0.5 M $SiCl_4$ at 20 mA cm^{-2} for 2 h at 100 °C and 2.76 × 10^6 Pa. As-deposited Si was etched in 5% HF solution for 30 s prior to electron microscopy analysis.

this method exhibited similar diffraction characteristics. Figure 2d shows an energy-dispersive X-ray (EDX) spectrum for the sample in Figure 2c. In this spectrum, only two signatures (Si K and Cu K) were observed above the background level, with the Cu K peak arising from the Cu TEM grid itself. The data in Figure 2d indicated that this grain was not a Si alloy/mixture with Ga, C, or Cl impurities at the level of detection (~0.1 atom %). EDX spectral measurements on the bulk material did show detectable Ga, but the difficulty in rigorously excluding Ga upon removal of the film from the electrode limited accurate ensemble assessment of the residual Ga content (Figure S10).

Taken together, the data presented here represent the first successful demonstration of an unassisted (i.e., no sonication,[28] no additional chemical reductant/template[29]) electrochemical process that produces crystalline Si in a single step under extremely mild conditions. The lowest temperature demonstrated here (80 °C) significantly bests both the previous reported record for direct electrodeposition of crystalline Si (745 °C in a fluoride melt electrolyte)[16] and more recent reports on the electrodeposition of Si through $CaSiO_3$ (850 °C in molten $CaCl_2$).[30] The electrodeposition temperatures shown here are also below the known temperature thresholds for metal-induced amorphous-to-crystalline Si transitions.[31]

In this work, the dissolved reducible species ($SiCl_4$), the electrolyte (TBACl), and the solvent (propylene carbonate) all are electrochemical components that have previously been explored separately and collectively in studies that universally yielded only amorphous Si.[5,7,13,32] Thus, the key innovation shown here is the specific use of Ga(*l*) as a liquid-metal electrode, consistent with ec-LLS at low temperatures. As described previously,[19−21] the ability of a liquid metal to act as a separate phase for recrystallization is a powerful and underutilized concept in electrochemistry. The present results are strong evidence in support of the contention that the ec-LLS approach can be exploited for the preparation of crystalline Si.

Further work is needed to advance the Si ec-LLS strategy as a practical and scalable wet-chemical process for the preparation of crystalline Si. The electrochemical reduction of $SiCl_4$ is not optimal at scale since $SiCl_4$ is readily hydrolyzed by water and is itself a high-energy-content, highly refined chemical. The reactivity of $SiCl_4$ toward trace water in the solvent is detrimental in the presented system since an insulating film that limits the progression of Si electrodeposition can develop. We observed this directly in prolonged electrodeposition experiments, where the masses of the crystalline Si films (i.e., after washing of the as-prepared films) increased with time for short (<1 h) experiments but were invariant with time in longer experiments because of a glassy coating on top of the crystalline Si film (Figure S11). Furthermore, $SiCl_4$ is prepared from Si rather than SiO_2, so this particular ec-LLS process parallels the Siemens process more than carbothermal reduction.[2] Nevertheless, further studies of Si ec-LLS with $SiCl_4$ in propylene carbonate should still be useful for understanding how the interplay of steps 2−4 in the Si ec-LLS process (Figure 1a) affects the resultant crystallinity/morphology. The results of such investigations should prove informative and general for the maturation of a viable ec-LLS process for crystalline Si that does use raw feedstock like silica. The electrochemical reduction of fully oxidized (low-energy-content) Si precursors in step 1 in Figure 1a also requires a more detailed and microscopic understanding of electrodepositions at liquid-metal electrodes. Such work is ongoing in our laboratory.

■ ASSOCIATED CONTENT

Supporting Information

Full description of the experimental methods and characterizations; optical photographs of the physical appearance of the collected electrodeposited material as a function of time; raw, as-collected X-ray diffraction patterns for electrodeposited crystalline Si at multiple temperatures; Raman spectra; and observations regarding the extent of electrodeposition over time. This material is available free of charge via the Internet at http://pubs.acs.org.

■ AUTHOR INFORMATION

Corresponding Author

smald@umich.edu

Notes

The authors declare no competing financial interest.

■ ACKNOWLEDGMENTS

Acknowledgment is made to the donors of the American Chemical Society Petroleum Research Fund (51339-DNI5) for support of this research. J.G. recognizes the University of Michigan Chemistry Department for a Research Excellence Award Fellowship. E.F. acknowledges a University of Michigan Rackham Merit Fellowship. The JEOL 3011 TEM instrument used in this work was maintained by the University of Michigan Electron Microbeam Analysis Laboratory through NSF support (DMR-0315633).

■ REFERENCES

(1) Tao, C. S.; Jiang, J.; Tao, M. *Sol. Energy Mater. Sol. Cells* **2011**, *95*, 3176−3180.
(2) Tao, M. *Interface* **2008**, *1*, 30−35.
(3) Elwell, D.; Feigelson, R. S. *Sol. Energy Mater.* **1982**, *6*, 123−145.

(4) Elwell, D.; Rao, G. M. *J. Appl. Electrochem.* **1988**, *18*, 15−22.
(5) Nishimura, Y.; Fukunaka, Y. *Electrochim. Acta* **2007**, *53*, 111−116.
(6) Munisamy, T.; Bard, A. J. *Electrochim. Acta* **2010**, *55*, 3797−3803.
(7) Agrawal, A. K.; Austin, A. E. *J. Electrochem. Soc.* **1981**, *128*, 2292−2296.
(8) Gobet, J.; Tannenberger, H. *J. Electrochem. Soc.* **1988**, *135*, 109−112.
(9) Takeda, Y.; Kanno, R.; Yamamoto, O.; Mohan, T. R. R.; Lee, C. H.; Kroger, F. A. *J. Electrochem. Soc.* **1981**, *128*, 1221−1224.
(10) Krishnamurthy, A.; Rasmussen, D. H.; Suni, I. I. *J. Electrochem. Soc.* **2011**, *158*, D68−D71.
(11) Nishimura, Y.; Nohira, T.; Morioka, T.; Hagiwara, R. *Electrochemistry* **2009**, *77*, 683−686.
(12) Nishimura, Y.; Fukunaka, Y.; Nishida, T.; Nohira, T.; Hagiwara, R. *Electrochem. Solid State Lett.* **2008**, *11*, D75−D79.
(13) El Abedin, S. Z.; Borissenko, N.; Endres, F. *Electrochem. Commun.* **2004**, *6*, 510−514.
(14) Komadina, J.; Akiyoshi, T.; Ishibashi, Y.; Fukunaka, Y.; Homma, T. *Electrochim. Acta* **2012**, DOI: 10.1016/j.electacta.2012.07.043.
(15) Oishi, T.; Watanabe, M.; Koyama, K.; Tanaka, M.; Saegusa, K. *J. Electrochem. Soc.* **2011**, *158*, E93−E99.
(16) Rao, G. M.; Elwell, D.; Feigelson, R. S. *J. Electrochem. Soc.* **1980**, *127*, 1940−1944.
(17) Cai, J.; Luo, X. T.; Haarberg, G. M.; Kongstein, O. E.; Wang, S. L. *J. Electrochem. Soc.* **2012**, *159*, D155−D158.
(18) Bieber, A. L.; Massot, L.; Gibilaro, M.; Cassayre, L.; Taxi, P.; Chamelot, P. *Electrochim. Acta* **2012**, *62*, 282−289.
(19) Carim, A. I.; Collins, S. M.; Foley, J. M.; Maldonado, S. *J. Am. Chem. Soc.* **2011**, *133*, 13292−13295.
(20) Gu, J.; Collins, S. M.; Carim, A.; Hao, X.; Bartlett, B.; Maldonado, S. *Nano Lett.* **2012**, *12*, 4617−4623.
(21) Fahrenkrug, E.; Gu, J.; Maldonado, S. *J. Am. Chem. Soc.* **2013**, *135*, 330−339.
(22) Olesinski, R. W.; Kanani, N.; Abbaschian, G. J. *Bull. Alloy Phase Diagrams* **1985**, *6*, 362−364.
(23) Trumbore, F. A. *Bell Syst. Tech. J.* **1960**, *39*, 205−233.
(24) Guminski, C. *J. Phase Equilib. Diffus.* **1999**, *20*, 344−346.
(25) Kearby, K. *J. Am. Chem. Soc.* **1936**, *58*, 374−375.
(26) Martinez, A. M.; Osen, K. S.; Kongstein, O. E.; Sheridan, E.; Ulyashin, A. G.; Haarberg, G. M. *ECS Trans.* **2010**, *25*, 107−118.
(27) McCreery, R. L. In *Electroanalytical Chemistry*, Vol. *17*; Bard, A. J., Ed.; CRC Press: Boca Raton, FL, 1990.
(28) Choi, J.; Wang, N. S.; Reipa, V. *Langmuir* **2009**, *25*, 7097−7102.
(29) Heath, J. R. *Science* **1992**, *258*, 1131−1133.
(30) Xiao, W.; Wang, X.; Yin, H.; Zhu, H.; Mao, X.; Wang, D. *RSC Adv.* **2012**, *2*, 7588−7593.
(31) Knaepen, W.; Detavernier, C.; Van Meirhaeghe, R. L.; Sweet, J. J.; Lavoie, C. *Thin Solid Films* **2008**, *516*, 4946−4952.
(32) Liu, X.; Zhang, Y.; Ge, D. T.; Zhao, J. P.; Li, Y.; Endres, F. *Phys. Chem. Chem. Phys.* **2012**, *14*, 5100−5105.